

Fluxional rearrangements in molybdenum(0), tungsten(0) and rhenium(I) carbonyl complexes of 2,6-bis[(4S)-isopropylloxazolin-2-yl]-pyridine (L). Crystal structure of $[\text{Mo}(\text{CO})_4\text{L}]^\ddagger$

Peter J. Heard *†^a and Derek A. Tocher^b

^a Department of Chemistry, Birkbeck College, Gordon House, 29 Gordon Square, London, UK WC1H 0PP

^b Department of Chemistry, University College London, Christopher Ingold Laboratories, 20 Gordon Street, London, UK WC1H 0AJ

Treatment of the $[\text{ReX}(\text{CO})_5]$ ($\text{X} = \text{Cl}, \text{Br}$ or I) and $[\text{M}(\text{CO})_4(\text{pip})_2]$ ($\text{M} = \text{Mo}$ or W , pip = piperidine) compounds with the C_2 -symmetric ligand 2,6-bis[(4S)-isopropylloxazolin-2-yl]pyridine (L) yielded complexes of general formulae *fac*- $[\text{ReX}(\text{CO})_3\text{L}]$ and *cis*- $[\text{M}(\text{CO})_4\text{L}]$, in which the ligand is co-ordinated in a bidentate fashion. In solution these complexes undergo a fluxional process that exchanges the co-ordinated and pendant oxazoline rings. In the case of the $\text{M}(\text{CO})_4$ complexes all permutational isomers are equivalent. However, in the rhenium(I) complexes the lower symmetry of the metal moiety leads to the formation of chemically distinct species. The different exchange pathways between these species gives rise to different magnetisation transfers, providing a spectroscopic handle on the mechanism of the ligand rearrangement. The activation parameters have been evaluated by standard one-dimensional band shape analysis and by two-dimensional exchange spectroscopy; ΔG^\ddagger (298 K) ≈ 52.0 and 62.6 kJ mol^{-1} , respectively for the complexes of Mo^0 and W^0 and is in the range 78.5 – 80.5 kJ mol^{-1} for the rhenium(I) complexes.

Complexes in which a meridional terdentate ligand has its bonding restricted to a bidentate mode of co-ordination are potentially fluxional.² The classical example of this type of fluxionality is exhibited by bidentate complexes of 2,2':6',2"-terpyridine (terpy), such as *fac*- $[\text{PtXMe}_3(\text{terpy})]$ ³ and *cis*- $[\text{Mo}(\text{CO})_4(\text{terpy})]$.⁴ In these complexes the ligand oscillates between equivalent bidentate forms *via* a mechanism that appears to involve the ligand adopting a pseudo-terdentate bonding mode in the transition state.^{3,4} To gain further insight into the mechanism of this type of fluxional exchange, we investigated the analogous complexes of the C_2 symmetric chiral ligand 2,6-bis[(4S)-methylloxazolin-2-yl]pyridine. The chiral centers on the ligand provide a spectroscopic handle on the mechanism, and it was shown that two independent exchange pathways were operative.¹

The question now arises as to how the energetics of these fluxional pathways are affected by the substituents on the oxazoline rings. To this end we now report on the solution-state stereodynamics of the molybdenum(0), tungsten(0) and rhenium(I) carbonyl complexes of the ligand 2,6-bis[(4S)-isopropylloxazolin-2-yl]pyridine (L), namely *cis*- $[\text{M}(\text{CO})_4\text{L}]$ ($\text{M} = \text{Mo}$ or W) and *fac*- $[\text{ReX}(\text{CO})_3\text{L}]$ ($\text{X} = \text{Cl}, \text{Br}$ or I).

Experimental

Syntheses

All manipulations were performed under an atmosphere of dry, oxygen-free nitrogen, using standard Schlenk techniques.⁵ Solvents were dried⁶ and degassed before use. The starting materials $[\text{M}(\text{CO})_4(\text{pip})_2]$ ($\text{M} = \text{Mo}$ or W , pip = piperidine)⁷ and $[\text{ReX}(\text{CO})_5]$ ($\text{X} = \text{Cl}, \text{Br}$ or I)⁸ and 2,6-bis[(4S)-isopropylloxazolin-2-yl]pyridine (L)⁹ were prepared by standard literature methods. The three rhenium complexes were prepared similarly, as illustrated by the procedure given for $[\text{ReBr}(\text{CO})_3\text{L}]$.

† E-Mail: p.heard@chem.bbk.ac.uk

‡ Dynamic stereochemical rearrangements in ‘chiral-at-ligand’ complexes. Part 2.¹

$[\text{CO}_3\text{L}]$. The molybdenum and tungsten complexes were prepared as illustrated by the procedure for $[\text{Mo}(\text{CO})_4\text{L}]$. Analytical data for the complexes are reported in Table 1.

{2,6-Bis[(4S)-isopropylloxazolin-2-yl]pyridine}bromotrichloronylrhenium(I). Pentacarbonylrhenium bromide (150 mg, 0.37 mmol) and 2,6-bis[(4S)-isopropylloxazolin-2-yl]pyridine (120 mg, 0.40 mmol) were refluxed in light petroleum (b.p. 60–80 °C)–benzene (2:1 v/v, 30 cm³) for *ca.* 18 h. The solvents were then concentrated to dryness *in vacuo*, to yield an orange oil. Crystallisation from CH_2Cl_2 –pentane gave 180 mg (75%) of $[\text{ReBr}(\text{CO})_3\text{L}]$.

{2,6-Bis[(4S)-isopropylloxazolin-2-yl]pyridine}tetracobonylmolybdenum(0). The complex $[\text{Mo}(\text{CO})_4(\text{pip})_2]$ (200 mg, 0.53 mmol) and 2,6-bis[(4S)-isopropylloxazolin-2-yl]pyridine (160 mg, 0.53 mmol) were stirred at ambient temperature for *ca.* 18 h in CH_2Cl_2 (20 cm³). The resulting red solution was concentrated to dryness *in vacuo*, and the solid residue recrystallised from CH_2Cl_2 –pentane to yield 180 mg (67%) of crystalline, red $[\text{Mo}(\text{CO})_4\text{L}]$.

Physical methods

Infrared spectra were recorded in CH_2Cl_2 using matched KBr solution cells, on a Nicolet 205 FT spectrometer, operating in the region 4000–400 cm^{−1}. Fast atom bombardment mass spectra were obtained at the London School of Pharmacy on samples of the complexes in a matrix of 3-nitrobenzyl alcohol, on a VG Analytical ZAB-SE instrument, using Xe^+ ion bombardment at 8 kV energy. Elemental analyses were carried out at University College London.

Hydrogen-1 NMR spectra were recorded in $(\text{CDCl}_3)_2$, CD_2Cl_2 or CDCl_3 on a Bruker AMX600 Fourier-transform spectrometer, at 600.13 MHz; chemical shifts are quoted relative to tetramethylsilane as an internal standard. Probe temperatures were controlled by a standard B-VT 2000 variable temperature unit; temperatures were checked against a standard sample of ethane-1,2-diol, and are considered accurate to

Table 1 Analytical data for the complexes $[M(CO)_4L]$ ($M = Mo$ or W) and $[ReX(CO)_3L]$ ($X = Cl$, Br or I)

Complex	Yield ^a (%)	$v(CO)^b/cm^{-1}$	m/z^c	Analysis ^d (%)		
				C	H	N
$[Mo(CO)_4L]$	67	1831, 1877, 1905, 2017	<i>e</i>	49.15 (49.53)	4.49 (4.55)	8.22 (8.25)
$[W(CO)_4L]$	75	1829, 1873, 1893, 2009	598 (M), 569 ($M - CO$), 541 ($M - 2CO$), 512 ($M - 3CO$)	41.55 (42.23)	3.72 (3.88)	6.86 (7.04)
$[ReCl(CO)_3L]$	82	1901, 1921, 2026	608 (M), 579 ($M - CO$), 544 ($M - Cl - CO$)	39.24 (39.57)	3.77 (3.81)	6.81 (6.92)
$[ReBr(CO)_3L]$	75	1903, 1923, 2026	652 (M), 623 ($M - CO$), 595 ($M - 2CO$), 572 ($M - Br$), 545 ($M - Br - CO$), 515 ($M - Br - 2CO$)	36.56 (36.87)	3.20 (3.56)	6.19 (6.45)
$[ReI(CO)_3L]$	79	1906, 1924, 2025	699 (M), 671 ($M - CO$), 544 ($M - I - CO$)	34.47 (34.39)	3.21 (3.32)	5.97 (6.02)

^a Relative to $[M(CO)_4(pip)_2]$ or $[ReX(CO)_5]$. ^b Recorded in CH_2Cl_2 . ^c FAB mass spectral data. ^d Calculated values in parentheses. ^e No diagnostically useful spectrum obtained (see text).

within ± 1 °C. Band shape analyses of the variable temperature spectra were carried out using the iterative simulation program DNMR 5.¹⁰ Two-dimensional exchange (EXSY) spectra were obtained using the Bruker program NOESYST, that generates the pulse sequence D1–90°–D0–90°–D8–90°–free induction decay. The relaxation delay, D1, was set at 2.0 s and the evolution time, D0, had an initial value of 3 μ s. The mixing time, D8, was varied between 0.01 and 1.0 s, according to the complex and experimental temperature. Spectra were collected typically with 256 words of data in t_1 and 4096 words of data in t_2 , and processed with 1024 words (data were forward linear predicted to 512 words, then zero-filled to 1024 words) in F_1 and 2048 words in F_2 (no zero filling). The spectral widths in F_1 and F_2 were *ca.* 9.6 ppm and sixteen scans were acquired for each of the 256 experiments. Rate data were extracted from the volume integrals of the resulting two-dimensional intensity matrix using the program D2DNMR.¹¹ Activation parameters were calculated from a least-squares fit of the linearised Eyring equation, using the rate data obtained from the band shape analyses or the EXSY spectra. The errors quoted are those defined by Binsch and Kessler.¹²

Crystallography

A single red crystal of $[Mo(CO)_4L]$ { $L = 2,6\text{-bis}[(4S)\text{-isopropylloxazolin-2-yl}]pyridine$ } with dimensions $0.66 \times 0.46 \times 0.40$ mm was obtained as described, and mounted on a glass fibre. All geometric and intensity data were taken from this sample by an automatic four-circle Nicolet R3 mV diffractometer, using the ω -2 θ technique, at 293(2) K. Three standard reflections (remeasured every 97 scans) showed no significant loss of intensity during data collection.

Crystal data and data collection parameters. $C_{21}H_{23}MoN_3O_6$, $M = 509.36$, orthorhombic, space group $P2_12_12_1$, Mo-K α radiation ($\lambda = 0.71073$ Å), $a = 9.519(2)$, $b = 13.394(3)$, $c = 18.316(4)$ Å, $U = 2335.2(9)$ Å³, $Z = 4$, $D_c = 1.449$ g cm⁻³, $\mu = 0.60$ mm⁻¹, $F(000) = 1040$, data collection range $5 < 2\theta < 50^\circ$, 2353 unique reflections collected.

Structure solution and refinement. Data were corrected for Lorentz-polarisation and absorption effects (empirically; ψ scan method; maximum transmission 0.92, minimum transmission 0.78). The structure was solved by direct methods (SHELXS 86),¹³ and developed using alternate cycles of least-squares refinement on F^2 and Fourier-difference synthesis (SHELXL 93).¹⁴ Non-hydrogen atoms were refined anisotropically, and hydrogen atoms placed in idealised positions [$r(C-H) = 0.96$ Å] and assigned a common isotropic thermal parameter. The final cycle of least squares included 281 parameters for the 2350 variables. The final R and $wR2$ values

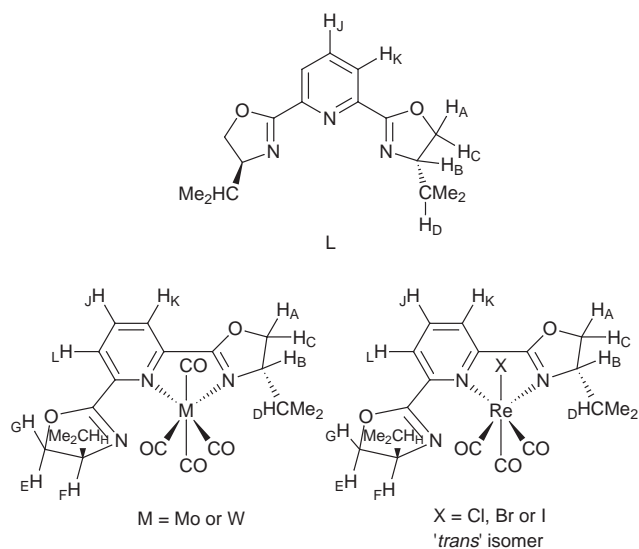


Fig. 1 The structures of the ligand 2,6-bis[(4S)-isopropylloxazolin-2-yl]pyridine (L), and the complexes $[M(CO)_4L]$ and $[ReX(CO)_3L]$, showing the H nuclide labeling scheme. Note that the $[ReX(CO)_3L]$ complexes form two chemically distinct isomers, and the structure depicted is that of the major ('*trans*') isomer (see text)

were 0.0330 and 0.0774, respectively [$I > 2\sigma(I)$, 2096 data], 0.0426 and 0.0880, for all data. The absolute configuration was determined unambiguously using SHELXL 93 procedures; calculated Flack parameter = 0.02(7).

CCDC reference number 186/1002.

Results

2,6-Bis[(4S)-isopropylloxazolin-2-yl]pyridine

2,6-Bis[(4S)-isopropylloxazolin-2-yl]pyridine (L) was prepared as described previously,⁹ and its absolute configuration confirmed by the crystal structure of $[Mo(CO)_4L]$ (see below). The full assignment of its 1H NMR spectrum L is necessary for the detailed analyses of the spectra of the complexes (see below); a discussion of this spectrum is therefore merited.

The ambient temperature (298 K) 1H NMR spectrum of 2,6-bis[(4S)-isopropylloxazolin-2-yl]pyridine in $CDCl_3$ shows signals in three regions. The isopropyl methyl environments are diastereotopic; thus the two equivalent isopropyl groups [free L has C_2 symmetry (Fig. 1)] give rise to a pair doublets, at δ 0.91 and 1.02 [$^3J(HH_D) \approx 6.8$ Hz], due to the methyls, and a multiplet, at δ 1.85, due to H_D (see Fig. 1 for labeling), which also couples to H_B of the oxazoline ring [$^3J(HH) = 6.4$ Hz]. The oxazoline-ring hydrogen nucleides give rise to three signals in a 1:1:1 intensity ratio, in the region δ 4.0–4.6: H_B gives a complex multiplet due to coupling to H_A , H_C and H_D , and H_A and

Table 2 Proton NMR chemical shift data^a for L and the complexes [M(CO)₄L] and [ReX(CO)₃L]

Compound ^b	Experimental conditions	δ (oxazoline-H)		δ (isopropyl-H)		δ (isopropyl-Me) ^c		δ (pyridine-H)	
		co-ordinated ring		unco-ordinated ring		major	minor	major	minor
		major	minor	major	major	minor	major	major	minor
Ligand	CDCl ₃ , 298 K			4.51 (H _A) 4.12 (H _B) 4.21 (H _C)	1.85 (H _D)		0.91 1.02	7.84 (H _J) 8.19 (H _K)	
[Mo(CO) ₄ L]	CD ₂ Cl ₂ , 200 K	4.68 (H _A) 4.43 (H _B) 4.57 (H _C)		4.74 (H _E) 4.31 (H _F) 4.20 (H _G)	1.86 (H _H) 2.52 (H _D)		0.74 (c) 0.92 (p) 0.95 (c) 0.99 (p)	7.79 (H _K or H _L) 7.89 (H _K or H _L) 8.05 (H _J)	
[W(CO) ₄ L]	(CDCl ₂) ₂ , 251 K	4.69 (H _A) 4.47 (H _B) 4.59 (H _C)		4.75 (H _E) 4.36 (H _F) 4.20 (H _G)	1.89 (H _H) 2.56 (H _D)		0.75 (c) 0.92 (p) 0.95 (c) 0.97 (p)	7.78 (H _K or H _L) 7.85 (H _K or H _L) 8.00 (H _J)	
[ReCl(CO) ₃ L]	(CDCl ₂) ₂ , 298 K (major = 88, minor = 12)	4.80 (H _A) 4.51 (H _B) 4.70 (H _C)	4.63 (H _B)	4.74 (H _E) 4.28 (H _F) 4.24 (H _G)	1.92 (H _H) 2.47 (H _D) 2.59 (H _D)	0.91 (c) 0.98 (p) 1.01 (c) 1.06 (p)	0.92 0.99 1.04	7.97 (H _K or H _L) 7.98 (H _K or H _L) 8.11 (H _J) 8.11 (H _J)	
[ReBr(CO) ₃ L]	(CDCl ₂) ₂ , 298 K (major = 94, minor = 6)	4.81 (H _A) 4.53 (H _B) 4.71 (H _C)	6.45 (H _B)	4.76 (H _E) 4.29 (H _F) 4.26 (H _G)	1.93 (H _H) 2.49 (H _D) 2.61 (H _D)	0.92 (c) 0.99 (p) 1.03 (c) 1.07 (p)	0.93 1.01 1.05	7.97 (H _K or H _L) 7.98 (H _K or H _L) 8.11 (H _J) 8.10 (H _J)	
[ReI(CO) ₃ L]	(CDCl ₂) ₂ , 298 K (major = 96, minor = 4)	4.81 (H _A) 4.55 (H _B) 4.71 (H _C)	4.50 (H _B) 4.66, ^d 4.64 ^e	4.76 (H _E) 4.30 (H _F) 4.26 (H _G)	1.95 (H _H) 2.50 (H _D) 2.62 (H _D)	0.92 (c) 0.99 (p) 1.03 (c) 1.07 (p)	0.94 0.95 1.05	7.96 (H _K or H _L) 7.99 (H _K or H _L) 8.10 (H _J) 8.10 (H _J)	7.93 (H _K) or H _L

^a See Fig. 1 for labeling; not all minor isomer resonances observed (see text). ^b Populations (%) of the two isomers given in parentheses. ^c c = co-ordinated, p = pendant; assignment of minor isomer signals to the pendant and co-ordinated oxazoline rings is uncertain. ^d H_C or H_E of the minor isomer. ^e H_C or H_E of the minor isomer.

Table 3 Proton NMR coupling constants^a for L and the complexes [M(CO)₄L] and [ReX(CO)₃L]

Coupling	Free L	[Mo(CO) ₄ L]	[W(CO) ₄ L]	[ReCl(CO) ₃ L]	ReBr(CO) ₃ L]	[ReI(CO) ₃ L]
$J(H_AH_B)$	9.7	10.4	10.4	10.4	10.4	10.4
$J(H_AH_C)$	7.8	9.1	8.8	9.2	9.1	9.1
$J(H_BH_C)$	8.4	7.1	6.5	7.6	7.5	7.5
$J(H_BH_D)$	6.4	3.3	3.1	3.6	3.6	3.6
$J(H_DH_{Me})^b$	6.8	6.9	7.1	6.9	6.8	6.8
$J(H_EH_F)$		10.2	10.1	9.0	9.2	9.5
$J(H_EH_G)$		8.2	8.2	7.4	7.4	7.7
$J(H_FH_G)$		8.5	8.2	9.3	9.0	8.9
$J(H_EH_H)$		6.7	6.1	6.7	6.4	6.5
$J(H_HH_{Me})^c$		6.8	6.7	6.7	6.8	6.9
$J(H_JH_K/H_L)$	7.7	8.0	7.8	7.9	7.9	7.9
$J(H_KH_L)$		0.9	1.3	1.2	1.4	1.4

^a Coupling constants in Hz; see Fig. 1 for labeling. Data for the [ReX(CO)₃L] complexes refer to the major isomer only (see text). ^b Co-ordinated isopropyl-methyls (average coupling to the two diastereotopic methyls). ^c Unco-ordinated isopropyl-methyls (average coupling to the two diastereotopic methyls).

H_C give rise to a doublet of doublets and a triplet, respectively; there is no evidence of any long range couplings between H_A and H_B or H_C and H_D. The assignments of H_A and H_C were made on the same basis as our assignments of the corresponding signals in 2,6-bis[(4S)-methylloxazolin-2-yl]pyridine.¹ Protons H_K and H_J (pyridine H) give rise to a doublet and a triplet, respectively, in the region δ 7.7–8.3. Hydrogen-1 NMR data are reported in Tables 2 and 3.

Complexes [M(CO)₄L]

The two complexes [M(CO)₄L] {M = Mo or W; L = 2,6-bis[(4S)-isopropylloxazolin-2-yl]pyridine} were obtained as red-brown crystalline solids, as described. The infrared spectra (CH₂Cl₂ solution) each display four carbonyl stretching bands in the region 2020–1820 cm⁻¹, characteristic of a *cis*-M(CO)₄ metal moiety,¹⁵ and the elemental analyses (Table 1) are consistent with the formula [M(CO)₄L]. Fast atom bombardment (FAB) mass spectrometry was carried out on both complexes. The tungsten complex displayed weak fragmentation peaks at

m/z = 598 [W(CO)₄L], 569 [W(CO)₃L], 541 [W(CO)₂L] and 512 [W(CO)L]; however, in the case of the molybdenum complex no diagnostically useful spectrum was obtained.

NMR studies. The ambient temperature ¹H NMR spectra of the complexes [M(CO)₄L] (M = Mo or W) displayed highly exchange-broadened signals. This broadening disappeared on cooling, and well resolved spectra were obtained at *ca.* 200 K for the molybdenum complex and *ca.* 250 K for the tungsten complex. The spectra of the two complexes were similar, and the results obtained for the tungsten complex, [W(CO)₄L], will serve to illustrate the analysis of the dynamic NMR problem.

The ¹H NMR spectrum of [W(CO)₄L] at 251 K in (CDCl₂)₂ showed signals characteristic of the ligand acting in a (non-exchanging) bidentate bonding mode (Fig. 1). The spectrum (Fig. 2) displayed signals in three regions: (i) the isopropyl region (*ca.* δ 0.7–2.6); (ii) the oxazoline-H region (*ca.* δ 4.1–4.8); (iii) the pyridine-H region (*ca.* δ 7.7–8.1). The isopropyl region of the spectrum displayed two pairs of doublets [³*J*(HH) ≈ 7

Hz], of equal intensity, due to two pairs of diastereotopic methyls, and two multiplets (also of equal intensity) due to the isopropyl hydrogens, H_D and H_H (Fig. 1). This points clearly to the ligand acting in an unsymmetrical bidentate bonding mode, with one oxazoline ring co-ordinated and the other unco-ordinated. The assignment of the methyl signals to the two oxazoline rings was made on the assumption^{16,17} that the chemical shift difference between the diastereotopic methyls of the co-ordinated ring would be greater than that between the diastereotopic methyls of the pendant ring. Thus the widely spaced pair of doublets was assigned to the isopropyl methyls of the co-ordinated oxazoline ring. The unsymmetrical bidentate bonding mode of the ligand renders all oxazoline-H nuclides inequivalent; thus the oxazoline-H region of the spectrum displays six equally intense signals. The signals can be assigned unambiguously to H_E , H_A , H_C , H_B , H_F and H_G , respectively, from high to low frequency by their relative chemical shifts [*c.f.* free L spectrum (see above)] and their scalar couplings (1H - 1H COSY experiment). The aromatic region of the spectrum displays a triplet, due H_J , and two doublets of doublets due to H_K

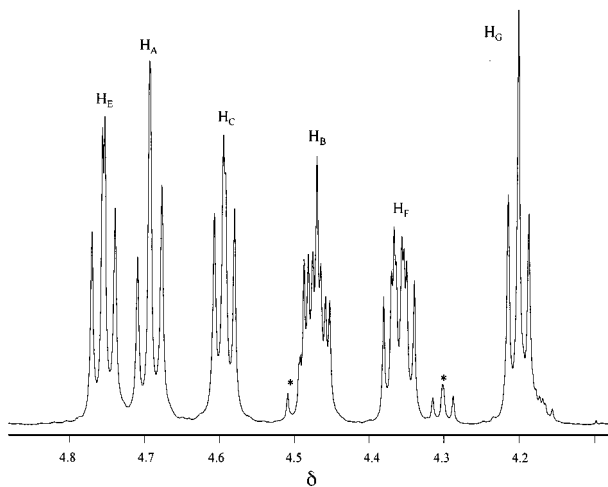
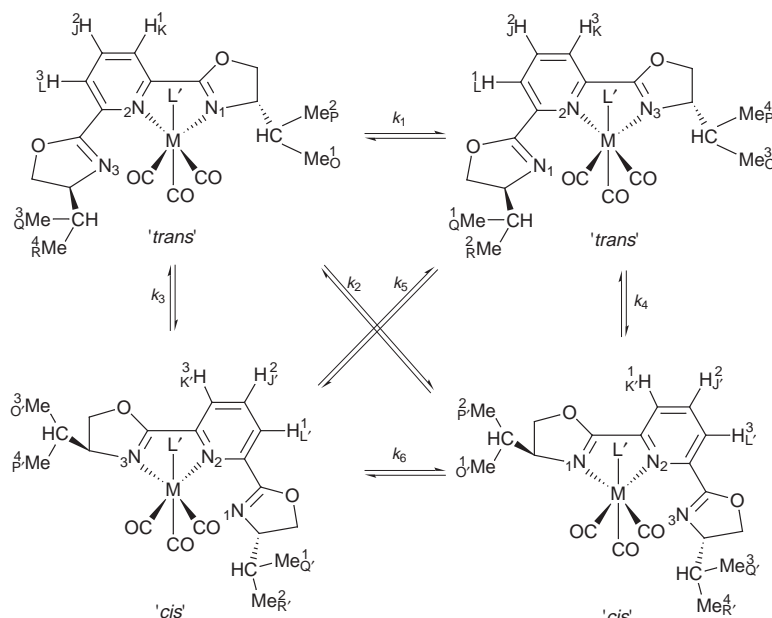
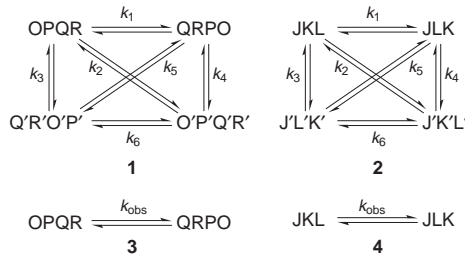


Fig. 2 The 600 MHz 1H NMR spectrum of $[W(CO)_4L]$ at 251 K, showing the oxazoline-H region. See Fig. 1 for labeling. The signals denoted * are due to decomposition

and H_L . Although it is not possible to distinguish unambiguously between H_K and H_L , this does not affect the analysis of the dynamic NMR problem (see below). Hydrogen-1 NMR data are reported in Tables 2 and 3.

On warming, fully reversible line shape changes were observed in all three regions of the spectrum (see above), due to the onset of a fluxional process on the NMR chemical shift timescale. The fluxional process leads to the exchange of analogous pairs of signals (*e.g.* H_K/H_L of the pyridine ring), clearly indicating an oscillation of the ligand between bidentate forms (Scheme 1). Four chemically indistinguishable permutational isomers, depicted in Scheme 1, exist in solution; these vary according to which oxazoline ring is co-ordinated, and the orientation of the isopropyl group of the co-ordinated oxazoline ring with respect to the axial M-CO groups. The fluxional process causes an interconversion of the isopropyl-Me and pyridine-H signals according to the dynamic spin systems **1** and **2**, respectively (see Scheme 1 for H atom labeling). Since all four species are degenerate, the spin systems reduce to **3** and **4**, respectively. The band shape changes associated with the isopropyl-methyl and pyridine-H signals were submitted to full analyses according to **3** and **4**. Although $[W(CO)_4L]$ is thermally unstable, fourteen reliable fits were obtained for the isopropyl-Me signals, and seventeen reliable fits were obtained on the pyridine-H signals. Five of the seventeen fits for the pyridine-H signals are shown in Fig. 3. In the case of the molybdenum complex, $[Mo(CO)_4L]$, only the pyridine-H signals were submitted to a total band shape analysis, and a total of fifteen reliable fits were obtained. The Eyring activation parameters for both complexes are reported in Table 4.

In analogous complexes of terpyridine, such as the tricarbonylrhenium(I) halide complexes, $[ReX(CO)_3(\text{terpy})]$ ($X = Cl, Br, I$,



Scheme 1 The four solution-state species of the complexes $[M(CO)_4L]$ ($M = Mo$ or W , $L' = CO$) and $[ReX(CO)_3L]$ ($L' = Cl, Br$ or I) and the interconversion pathways between them. The labels 'cis' and 'trans' refer to the orientation of the co-ordinated oxazoline ring isopropyl group with respect to the axial ligand, L' . Note that the 'cis' and 'trans' species are chemically equivalent in the $[M(CO)_4L]$ complexes ($L = L'$), but not in the $[ReX(CO)_3L]$ complexes ($L \neq L'$).

Table 4 Eyring activation parameters^a for the complexes $[M(CO)_4L]$ and $[ReX(CO)_3L]$

Complex	Fluxional process ^b	$\Delta H^\ddagger/kJ\ mol^{-1}$	$\Delta S^\ddagger/J\ K^{-1}\ mol^{-1}$	$\Delta G^\ddagger/kJ\ mol^{-1}$
$[Mo(CO)_4L]$	'Tick-tock twist' ^c	55(1)	10(4)	52.04(17)
$[W(CO)_4L]$	'Tick-tock twist' ^c	61.5(6) ^d	-4(2) ^d	62.53(3) ^d
$[W(CO)_4L^2]'$ ^f	'Tick-tock twist' ^c	70(2) ^e	24(7) ^e	62.69(8) ^e
$[ReCl(CO)_3L]$	'Tick-tock twist' ^g	73(1)	-21(4)	78.98(5)
$[ReBr(CO)_3L]$	'Tick-tock twist' ^g	71(1)	-32(4)	80.26(5)
$[ReI(CO)_3L]$	'Tick-tock twist' ^g	69.2(4)	-36(1)	79.79(1)

^a ΔG^\ddagger quoted at 298 K; errors in parentheses. ^b See text. ^c Probable mechanism, see text. ^d From band shape analysis of the pyridine-H signals. ^e From band shape analysis of the isopropyl-Me signals. ^f $L^2 = 2,6\text{-Bis}(4S)\text{-methylloxazolin-2-yl}]\text{pyridine}$; ΔG^\ddagger determined from band coalescence (pyridine-H signals), $T_c \approx 298$ K; estimated error ca. $\pm 10\%$. ^g Data refer to the major —> minor isomer process.

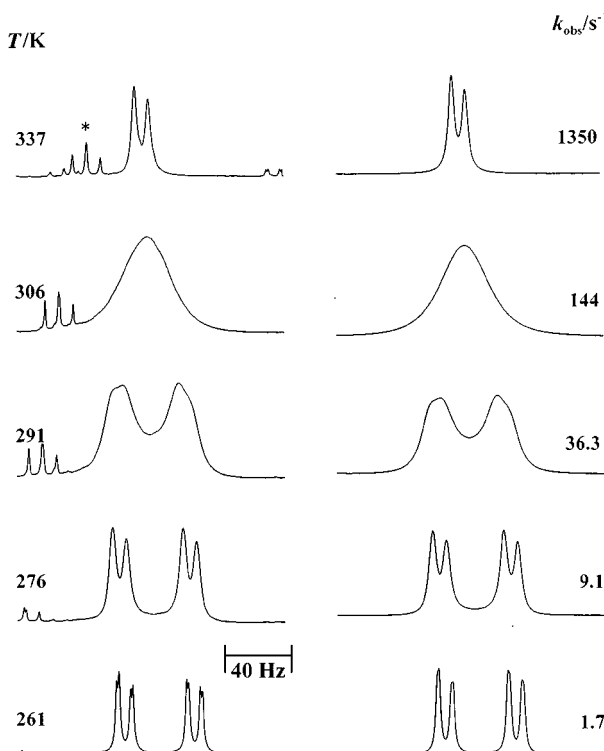


Fig. 3 Variable temperature and computer-simulated ^1H NMR spectra of $[W(CO)_4L]$, showing the pyridine-H region. The 'best-fit' rate constants, k_{obs} , for the ligand rearrangement are shown alongside. Rate data for the other temperatures are: $k_{obs}/\text{s}^{-1} = 0.7$ (255), 3.4 (266), 5.9 (271), 14.8 (281), 23.5 (286), 56.9 (296), 90.6 (301), 205 (311), 280 (316), 405 (321), 630 (327) and 890 (332 K). The signal denoted * is due to decomposition

Br or I), restricted rotation of pendant pyridine ring has been observed by low temperature NMR studies.¹⁸ Samples of the complexes, $[M(CO)_4L]$ ($M = Mo$ or W) were therefore cooled to ca. 180 K (CD_2Cl_2 solution), to investigate the possibility of hindered rotation of the pendant oxazoline ring. However, the spectra remained essentially unchanged below the low temperature limit of the ligand fluxion (see above). It is possible that rotation about the C (pyridine)-C (oxazoline) bond is rapid (on the NMR timescale) at these temperatures; however, this is considered unlikely, and we tend to the view that the ^1H NMR spectra are insensitive to the restricted motion as a consequence of the pendant oxazoline ring adopting either chemically indistinct rotamers, or a single rotameric form. This also appears to be the case in the rhenium(I) complexes, $[ReX(CO)_3L]$ { $X = Cl$, Br or I; $L = 2,6\text{-bis}(4S)\text{-isopropylloxazolin-2-yl}]\text{pyridine}$ } (see below).

Attempts to isolate the analogous complexes of 2,6-bis($4S$)-methylloxazolin-2-yl]pyridine (L^2), namely $[M(CO)_4L^2]$ ($M = Mo$ or W), and study their stereodynamics were frustrated by

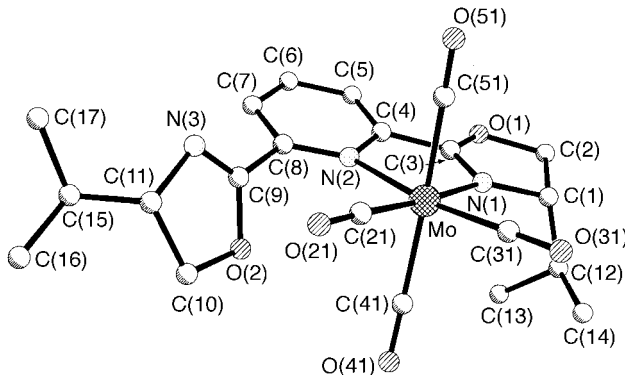


Fig. 4 Molecular structure of $[Mo(CO)_4L]$, showing the atom labeling scheme. Hydrogen atoms omitted for clarity

their instability. Infrared and ^1H NMR spectroscopy indicated the formation of the desired species from reactions of the $[M(CO)_4(\text{pip})_2]$ compounds ($M = Mo$ or W , pip = piperidine) with a stoichiometric quantity of the ligand; however analytically pure samples could not be obtained and the ^1H NMR spectra were complicated by the presence of resonances due to decomposition products. An approximate value for the free energy of activation, ΔG^\ddagger , for the ligand fluxion was obtained for $[W(CO)_4L^2]$, from coalescence temperature measurements (pyridine-H signals) (Table 4). However, no kinetic data could be obtained for the molybdenum complex $[Mo(CO)_4L^2]$.

Crystal structure of $[Mo(CO)_4L]$. The crystal structure of $[Mo(CO)_4L]$ was obtained primarily to verify the bidentate bonding mode of the ligand, and to confirm the absolute configuration of the ligand at C(1) and C(11). A view of the molecule showing the atom numbering scheme is shown in Fig. 4, and selected bond lengths and angles are reported in Table 5. Fig. 4 shows that the molecule has the expected *cis*-octahedral co-ordination geometry, with the ligand acting in a bidentate bonding mode. The geometry at the metal centre deviates somewhat from that of an idealised octahedron, due to the small bite angle of the ligand $N(1)-Mo-N(2)$ 72.3°. The dihedral angle between the pendant ring and the plane containing $N(1)-Mo-N(2)$ is 55.7°, which compares to 76.2 and 52.9° respectively for the analogous dihedral angles in the complexes $[ReCl(CO)_3L^2]$ ¹ and $[ReBr(CO)_3(\text{terpy})]$.¹⁸ There are no significant differences in bond lengths between the pendant and coordinated oxazoline rings. The absolute configuration at C(1) (*S*) and C(11) (*S*) was confirmed.

Complexes $[ReX(CO)_3L]$

The three complexes $[ReX(CO)_3L]$ { $X = Cl$, Br or I; $L = 2,6\text{-bis}(4S)\text{-isopropylloxazolin-2-yl}]\text{pyridine}$ } were prepared as described (see above), and isolated as air-stable orange crystalline solids. The infrared spectra (CH_2Cl_2) of all three complexes display three bands in the carbonyl stretching region of the

Table 5 Selected bond lengths (\AA) and angles ($^\circ$) for $[\text{Mo}(\text{CO})_4\text{L}]$

Mo–C(21)	1.963(7)	N(1)–C(3)	1.284(7)
Mo–C(31)	1.960(6)	N(2)–C(4)	1.365(7)
Mo–C(41)	2.050(7)	N(3)–C(9)	1.259(8)
Mo–C(51)	2.070(7)	O(1)–C(3)	1.343(7)
Mo–N(1)	2.284(4)	O(2)–C(9)	1.380(7)
Mo–N(2)	2.351(4)	C(3)–C(4)	1.486(9)
C(31)–Mo–C(21)	86.8(3)	C(3)–N(1)–Mo	115.0(4)
C(41)–Mo–C(51)	169.3(2)	N(1)–C(3)–C(4)	122.3(5)
C(21)–Mo–N(1)	174.4(2)	N(2)–C(4)–C(3)	113.9(5)
C(21)–Mo–N(2)	102.2(2)	C(4)–N(2)–Mo	113.8(4)
C(31)–Mo–N(1)	98.7(2)	N(1)–C(3)–O(1)	120.2(6)
C(31)–Mo–N(2)	169.8(2)	N(3)–C(9)–O(2)	119.3(5)
N(1)–Mo–N(2)	72.3(2)	C(1)–C(12)–C(13)	112.1(6)

spectrum characteristic of a *fac*-octahedron tricarbonyl coordination geometry.¹⁹ This clearly indicates that the ligand is bound in a bidentate fashion. Elemental analyses and FAB mass spectral data are also consistent with the presence of $[\text{ReX}(\text{CO})_3\text{L}]$ (X = Cl, Br or I). Analytical data are reported in Table 1.

NMR studies. The ambient temperature (298 K) ^1H NMR spectra [$(\text{CDCl}_2)_2$ solution] of the complexes, displayed well resolved signals due to the presence of two isomers of widely differing populations (see below). The spectra were essentially identical for the three complexes, and discussion of the chloro complex, $[\text{ReCl}(\text{CO})_3\text{L}]$, will serve to illustrate the analysis of the problem.

The ^1H NMR spectrum of $[\text{ReCl}(\text{CO})_3\text{L}]$ at 298 K displayed two sets of signals of different intensities, due to the presence of two isomers, that vary according to the orientation of the co-ordinated oxazoline-isopropyl group with respect to the halogen [L' (Scheme 1)]; the relative populations of the two species (see below) are 1:7. The assignment of the two sets of signals was made on the basis that the ‘*cis*’ isomer (Scheme 1) would be disfavoured on steric grounds. Although this hypothesis is supported by the decrease in the population of minor species with increasing size of the halogen (Table 2), some caution is necessary in this assignment because, in the analogous complexes of 2,6-bis[(4S)-methyloxazolin-2-yl]pyridine, the methyl group of the co-ordinated oxazoline is oriented ‘*cis*’ to the halogen in the solid state.¹ This indicates that any steric interactions between the methyl and the halogen are minimal. However, it is thought likely that the increased steric requirements of the isopropyl group (compared to the Me group) in the present complexes would favour the ‘*trans*’ species; the latter was therefore assigned as the major isomer.

The ‘static’ ^1H NMR spectrum of $[\text{ReCl}(\text{CO})_3\text{L}]$ was exactly analogous to that of $[\text{W}(\text{CO})_4\text{L}]$ (see above), except for the presence of the additional signals due to the minor isomer, and spectral assignments were made similarly. A full assignment of minor isomer resonances was frustrated by the low population and the small chemical shift differences between the two sets of signals. The scalar couplings of the minor isomer were not measured, but are presumably similar to those of the major isomer (Table 3). The relative populations of the two isomers were determined by integration of isopropyl-H signals of the co-ordinated oxazoline rings. Hydrogen-1 NMR data for the complexes $[\text{ReX}(\text{CO})_3\text{L}]$ (X = Cl, Br or I) are reported in Tables 2 and 3.

On warming above *ca.* 310 K the signals due to the minor species quickly broadened, as a result of a dynamic chemical exchange process that involves an oscillation of the ligand between bidentate bonding modes (Scheme 1). As a consequence of the extensive overlap of the signals due to the two isomers (see above), the only signals amenable to analysis are those of the isopropyl-H nuclides. However, these signals cannot be accurately simulated because of their complexity.

Table 6 Two-dimensional EXSY data for the complexes $[\text{ReX}(\text{CO})_3\text{L}]$

Complex	T/K	Mixing time, D8/s	k^*/s^{-1}
$[\text{ReCl}(\text{CO})_3\text{L}]$	293	1.000	0.049
	298	0.650	0.094
	303	0.400	0.154
	308	0.250	0.242
	313	0.150	0.372
	318	0.100	0.624
	323	0.060	0.933
	329	0.035	1.487
$[\text{ReBr}(\text{CO})_3\text{L}]$	293	0.900	0.031
	298	0.300	0.054
	303	0.150	0.082
	308	0.100	0.145
	313	0.060	0.225
	318	0.090	0.372
	323	0.020	0.496
	329	0.010	0.829
$[\text{ReI}(\text{CO})_3\text{L}]$	288	1.000	0.024
	293	0.600	0.040
	298	0.300	0.063
	303	0.180	0.103
	308	0.100	0.163
	313	0.060	0.262
	318	0.035	0.403
	323	0.022	0.596

* First-order rate constants for the major \longrightarrow minor isomer fluxional process. Uncertainties are *ca.* $\pm 5\%$.

Kinetic data for the fluxional process were therefore obtained by two-dimensional exchange spectroscopy.

Each isomer gives rise to a degenerate pair of (chemically indistinguishable) species in solution (Scheme 1); thus there are four species in solution, and three possible independent exchange pathways between them. Eight EXSY spectra were recorded at *ca.* 5 K intervals between 293 and 329 K (Table 6). Over this temperature range, exchange only occurs between the two isomers, along pathways k_3 and k_4 (Scheme 1); rates along the other two pathways, $k_1 (= k_6)$ and $k_2 (= k_5)$, are negligible (see below). This can be clearly seen in the two-dimensional EXSY spectrum of $[\text{ReCl}(\text{CO})_3\text{L}]$ at 308 K (Fig. 5), where cross-peaks only occur between the signals of the pendant and co-ordinated isopropyl-H of different isomers. Accurate rate data for the dynamic process were obtained from the EXSY spectra and are reported in Table 6. The Eyring activation parameters are in Table 4.

In a previous study by our group on the analogous tricarbonylrhenium(I) halide complexes of 2,6-bis[(4S)-methyloxazolin-2-yl]pyridine¹ it was shown that, at higher temperatures, the so-called ‘rotation’ pathway (see below) [pathway $k_1 (= k_6)$, Scheme 1] was also operative. To investigate whether or not the ‘rotation’ pathway also occurs in the present complexes a full set of variable temperature ^1H NMR spectra were acquired between ambient temperature (298 K) and *ca.* 410 K [the upper working limit for $(\text{CDCl}_2)_2$ solutions]. The spectra displayed the expected band shape changes due to the isomer exchange, but did not reveal any conclusive evidence of magnetisation transfer *via* pathway $k_1 (k_6)$. However, some reversible broadening of the pyridine-H resonances, H_K and H_L that could be attributable to magnetisation transfer along $k_1 (k_6)$, was observed as the high temperature limit was approached.

A low temperature ^1H NMR study (CD_2Cl_2 solution) was carried out, to investigate the possibility of restricted rotation of the pendant oxazoline ring about the C (pyridine)–C (oxazoline) bond. As in the molybdenum and tungsten complexes (see above), no evidence of any hindered rotation was observed. Again, this was attributed to the pendant oxazoline ring adopting either chemically indistinct rotamers, or a single rotameric form, rather than the rotation remaining rapid at low temper-

atures (see above). This is also in accord with the results of a previous study on the tricarbonylrhenium(I) halide complexes of 2,6-bis[(4S)-methyloxazolin-2-yl]pyridine.¹

Discussion

Fluxional processes

The two (generally accepted) possible mechanisms of the ligand fluxion in complexes of this type have been discussed previously,^{1,3,4,18,20} and are depicted in Scheme 2. For the tricarbonylrhenium(I) halide complexes of 2,6-bis[(4S)-isopropylloxazolin-2-yl]pyridine it is possible to distinguish between these two mechanisms because they give rise to different, observable magnetisation transfers.¹ Two-dimensional EXSY experiments (see above) reveal that the only observable magnetisation transfers occur along pathways k_3 and k_4 , which are identical (Scheme 1). These two fluxional pathways arise as a consequence of the so called 'tick-tock twist' mechanism [Scheme 2 (ii)], indicating that this mechanism is operative in these complexes at moderate temperatures. In a previous study on the analogous complexes of 2,6-bis[(4S)-methyloxazolin-2-yl]pyridine,¹

band shape analysis of the oxazoline-Me signals indicated that the so-called 'rotation' mechanism [Scheme 2 (i)] was also operative at higher temperatures. There is some evidence to indicate that this mechanism might also occur at high temperatures (above *ca.* 400 K) in the present complexes (see above); however, since higher temperature studies were not attempted this could not be demonstrated conclusively.

A third possible mechanism has been suggested by Rotondo *et al.*²¹ for the analogous ligand fluxion observed in square-planar complexes of Pd^{II} and Pt^{II} with terpyridine, namely *cis*-[M(C₆F₅)₂(terpy)]. An equivalent mechanism can also be envisaged for octahedral complexes of the type reported here.¹ Such a mechanism gives rise to the same magnetisation pathways as the 'tick-tock twist' mechanism (*i.e.* pathways k_3 and k_4 , Scheme 1); however, if this mechanism were operative, free rotation about the M–N (pyridine) bond would be expected to occur in the intermediate. This would lead to observable magnetisation transfers along pathways k_2 and k_5 . Rates along pathways k_2 and k_5 are clearly negligible at moderate temperatures (EXSY data), indicating that the ligand fluxion occurs *via* a 'tick-tock twist' mechanism rather than a 'Rotondo-type' mechanism. Entropy of activation data are consistent with this interpretation (see below).

Since all four permutational isomers are degenerate in the [M(CO)₄L] (M = Mo or W) complexes, the different fluxional pathways cannot be differentiated; all give rise to the same ¹H NMR magnetisation transfers. In principle, the presence (or otherwise) of the 'tick-tock twist' mechanism could be probed by ¹³C NMR studies; the equatorial M–CO environments would be exchanged if the ligand fluxion occurred *via* this mechanism. However, the instability of the complexes frustrated attempts to acquire ¹³C NMR spectra of sufficient quality to investigate the effects of the fluxion on the M–CO signals. Since these complexes are closely analogous to the rhenium complexes, we tend to the opinion that the 'tick-tock twist' mechanism is likely to be operative. The possibility of the rotation mechanism also occurring is an intriguing one. Its contribution to the overall ligand rearrangement in complexes of the type reported here will (presumably) be influenced by the relative strengths of the M–N (oxazoline) bonds (see below). Molybdenum- and tungsten–nitrogen (oxazoline) bonds are expected to be weaker than the corresponding Re–N (oxazoline) bonds; the rate of exchange *via* the 'rotation' pathway might, therefore, be expected to be greater for the complexes of Mo and W than for Re. Thus, some contribution from the 'rotation' pathway to the observed rate constant, k_{obs} , for the ligand fluxion in the [M(CO)₄L] complexes cannot be ruled out, and further studies are necessary to probe this possibility; such studies are currently in progress in our laboratories.

Activation parameters

Examination of the activation parameters obtained for the complexes (Table 4) reveals several interesting points.

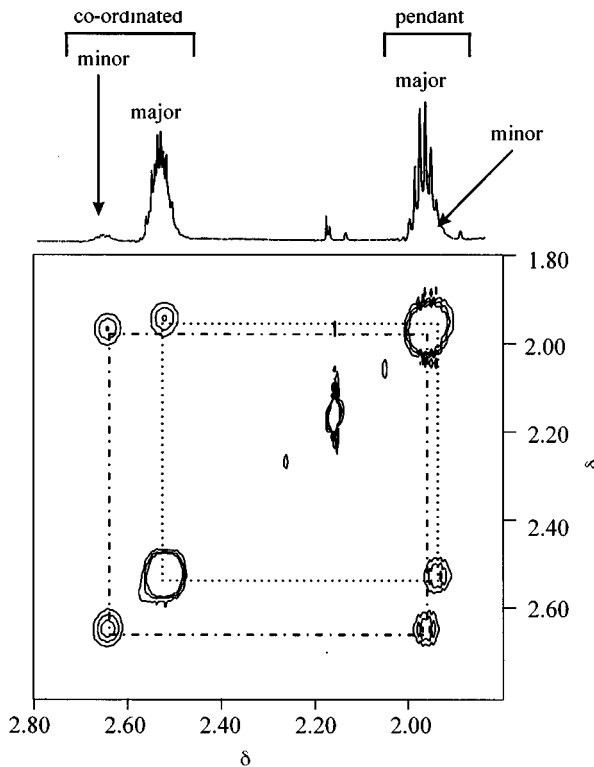
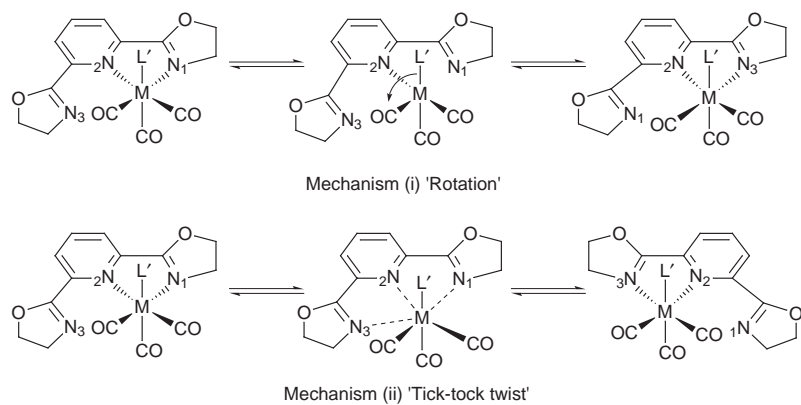


Fig. 5 Two-dimensional exchange spectrum of [ReCl(CO)₃L] at 308 K, showing exchange between the co-ordinated and pendant isopropyl-H environments of the different isomers



Scheme 2 The two possible mechanisms of the fluxional processes in the complexes [M(CO)₄L] and [ReX(CO)₃L]

(i) The trend in the free energy of activation, ΔG^\ddagger (298 K), with respect to the metal moieties is $\text{Re}^{\text{I}} > \text{W}^{\text{0}} > \text{Mo}^{\text{0}}$, which is in line with the trends reported previously for fluxional rearrangements of this type.⁴ However, the absolute magnitudes for ΔG^\ddagger (298 K) are the highest reported thus far for these metals for this type of rearrangement.^{1,4,22} The high magnitudes for ΔG^\ddagger presumably arise as a consequence of the formation of strong M–N (oxazoline) bonds.

(ii) The free energies of activation for ‘tick-tock twist’ rearrangement in the $[\text{ReX}(\text{CO})_3\text{L}]$ complexes are *ca.* 5.5 kJ mol⁻¹ higher than for the corresponding complexes of the ligand and 2,6-bis[(4S)-methyloxazolin-2-yl]pyridine.¹ This indicates that the Re–N (oxazoline) bond is several kJ mol⁻¹ stronger in the 4-isopropylloxazolinyl complexes than in the 4-methyl-oxazolinyl complexes, despite the increased steric requirements of the ligand. The formation of stronger Re–N (oxazoline) bonds in the present complexes presumably accounts for the negligible contribution of the ‘rotation’ mechanism (which necessarily involves its cleavage) to the overall stereodynamics.

(ii) Although entropies of activation are subject to considerable errors, and should only be viewed with caution, it is apparent that ΔS^\ddagger is negative for the rearrangement in the rhenium(I) complexes [ΔS^\ddagger (average) $\approx -30 \text{ J K}^{-1} \text{ mol}^{-1}$]. This is consistent with a ‘tick-tock twist’ rather than a ‘Rotondo-type’ mechanism; the transition state in the ‘tick-tock twist’ mechanism is considerably more ordered than in the ‘Rotondo-type’ mechanism.^{1,21} For the $\text{M}(\text{CO})_4$ complexes, entropies of activation [ΔS^\ddagger (average) $\approx 10 \text{ J K}^{-1} \text{ mol}^{-1}$] are also in accord with an ordered transition state, indicating that the largest contribution to the observed rate constant (see above) comes from exchange along the ‘tick-tock twist’ pathways, k_3 and k_4 (Scheme 1).

Acknowledgements

P. J. H. is grateful to Birkbeck College, for financial support, and to the University of London Intercollegiate Research Service for access to the NMR facilities at Queen Mary and Westfield College. Dr. H. Toms and Mr. P. Haycock are acknowledged for the acquisition of the NMR spectra.

References

- Part 1, P. J. Heard and C. Jones, *J. Chem. Soc., Dalton Trans.*, 1997, 1083.
- E. W. Abel and K. G. Orrell, *Encyclopedia of Inorganic Chemistry*, ed. R. B. King, Wiley, New York, 1994, vol. 5.
- E. W. Abel, V. S. Dimitrov, N. J. Long, K. G. Orrell, A. G. Osborne, V. Šík, M. B. Hursthouse and M. A. Mazid, *J. Chem. Soc., Dalton Trans.*, 1993, 291.
- E. W. Abel, K. G. Orrell, A. G. Osborne, H. M. Pain and V. Šík, *J. Chem. Soc., Dalton Trans.*, 1994, 111.
- D. F. Shriver, *Manipulation of Air-sensitive Compounds*, McGraw-Hill, New York, 1969.
- D. D. Perrin and W. L. F. Armarego, *Purification of Laboratory Chemicals*, Pergamon, Oxford, 1988.
- D. J. Dahrenbourg and R. L. Kump, *Inorg. Chem.*, 1978, **17**, 2680.
- S. P. Schmidt, W. C. Troglar and F. Basolo, *Inorg. Synth.*, 1979, **28**, 160.
- H. Nishiyama, M. Kondo, T. Nakamura and K. Itoh, *Organometallics*, 1991, **10**, 500.
- D. S. Stephenson and G. Binsch, DNMR 5, Quantum Chemistry Program Exchange, Indiana University, 1978.
- E. W. Abel, T. P. J. Coston, K. G. Orrell, V. Šík and D. Stephenson, *J. Magn. Reson.*, 1986, **70**, 34.
- G. Binsch and H. Kessler, *Angew. Chem., Int. Ed. Engl.*, 1980, **19**, 411.
- G. M. Sheldrick, *Acta Crystallogr., Sect. A*, 1990, **46**, 467.
- G. M. Sheldrick, SHELXL 93, University of Göttingen, 1993.
- L. E. Orgel, *Inorg. Chem.*, 1962, **1**, 25.
- H. Nishiyama, S. Yamaguchi, S.-B. Park and K. Itoh, *Tetrahedron Asymmetry*, 1993, **4**, 143.
- H. Nishiyama, S.-B. Park, M. Haga, K. Aoki and K. Itoh, *Chem. Lett.*, 1994, 1111.
- E. W. Abel, V. S. Dimitrov, N. J. Long, K. G. Orrell, A. G. Osborne, H. M. Pain, V. Šík, M. B. Hursthouse and M. A. Mazid, *J. Chem. Soc., Dalton Trans.*, 1993, 597.
- D. A. Edwards and J. Marshalsea, *J. Organomet. Chem.*, 1977, **131**, 73.
- E. W. Abel, A. Gelling, K. G. Orrell, A. G. Osborne and V. Šík, *Chem. Commun.*, 1996, 2329.
- E. Rotondo, G. Giordano and D. Minniti, *J. Chem. Soc., Dalton Trans.*, 1996, 253.
- A. Gelling, K. G. Orrell, A. G. Osborne, V. Šík, M. B. Hursthouse and S. J. Cole, *J. Chem. Soc., Dalton Trans.*, 1996, 203.

Received 13th February 1998; Paper 8/01264D